Failure evaluation of composite concrete using an acoustic emissions technique

Failure evaluation of composite concrete using an acoustic emissions technique

Safaa Kh Al-Jumaili[1], Ahmad K Jassim[2] and Dhia C Ali[1]

[1, 3] Materials Engineering Department, College of Engineering, University of Basrah, Basrah, Iraq
[2] Research and Development Department, the State Company for Iron and Steel, Basrah, Iraq

E-mail: safaakh@gmail.com

Abstract. One major problem with concrete is high brittleness with low tensile strength and strain capacity, which can cause sudden failure. Structural Health Monitoring (SHM) is thus very important to detect cracks in initial stages to avoid catastrophic failure. In this research, an acoustic emissions (AE) technique was applied to enable SHM to detect cracks and predict the failure of composite concrete. This physical non-destructive testing process utilises transient elastic waves caused by the rapid release of energy from a localised source within a structure. A low-frequency acoustic emission system was thus tested for economical monitoring of the damage to reinforced composite cubic concrete under compression. Specimens of standard size (150 x 150 x 150 mm) were produced without and with polyamide reinforcement bars. The compression strength of the cubic concrete was then tested according to BS EN 12390-1. Prior to testing, a low-cost single piezoelectric wafer active sensor was applied to the centre of one side of each specimen, which was then connected to a PC's sound card. Data was successfully recorded using sensors and the real-time of the applied load was recorded using a separate data logger. Traditional AE signal parameters were extracted and used for damage evaluation. The results indicated that the AE system was capable of detecting cracks in representative structures to final failure. Signal amplitude with load versus time showed an increase in AE activity and energy approaching the end of the test, while commutative hits could be used to distinguish between stable and unstable loading stages. The system also detected the initiation of the final failure stage at 72.6% and 83% of the failure load of specimens without and with polyamide reinforcement bars, respectively.

Keywords: Failure evaluation, Composite concrete, Acoustic Emission, Structural Health Monitoring.

1. Introduction

Concrete can be damaged in several different manners, from the micro-cracking level to structural fractures. Cracks in concrete may occur when the structure is under a loading regime or even where there is no loaded situation, and thus regular inspection is required to examine the integrity of structures. These are generally applied in order to reveal the damage level and deterioration of a structure [1], yet using traditional inspection techniques (such as visual inspection) does not allow assessment of the deteriorating performance in many structures because they cannot detect internal fractures or reach

inaccessible locations [2]. Structural health monitoring (SHM) techniques must thus be used in order to overcome this problem and increase the structure reliability and safety. In particular, using fully integrated transducers within the structure allows real-time data about structural integrity to be determined, providing the operator with early-warning signals that may allow limitation or prevention of losses associated with final collapse [3-6].

In general, SHM offers three levels of monitoring: (a) detection of initial damage and damage location; (b) estimation of the extent of damage; and (c) predictions of remaining life for the structure [7-9]. The acoustic emissions (AE) technique is an effective SHM technique whereby piezoelectric transducers are used to detect elastic stress waves emitted by damage growth [10]. The AE technique thus offers a way to detect [11], locate [12-14] and characterise [15-17] damage within a structure. Each AE signal is recorded as a waveform; the main features of the AE signal are shown in Figure 1 [18].

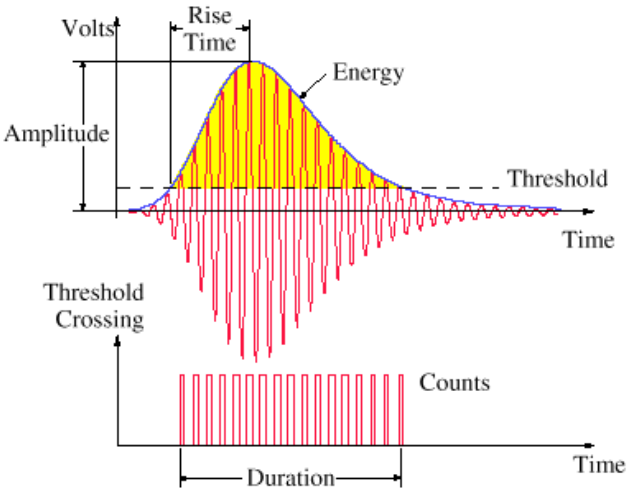

Figure 1. The main features of an AE signal [18].

AE has now been adopted as an effective non-destructive technique to monitor composite materials such as concrete [19-24], and evaluation of concrete structures' degradation using the AE technique has been reported in many research studies [19-21]. Traditional AE methods based on AE rate analysis have been proven to be applicable for estimating the degree of damage in concrete under different environmental conditions [25, 26], yet this conventional AE technique has various drawbacks, such as its expense and the need for huge quantities of data storage, especially for long term monitoring. This has made it vital to develop new low-frequency and cost-effective AE monitoring systems.

Piezoelectric materials are generally low cost and they are thus widely used as transducers in the SHM field [27]. The fact that piezoelectric impact is a reversible process can be described using the phenomenon where the electrical charge is converted into a strain (deformation), so that the applied stress generates electric charges in the material, while conversely, deformation in the piezoelectric material's geometry occur where an electric field is applied [28].

The aim of this work was to examine a simple data acquisition system to develop a cost-effective process using piezoelectric wafer active sensors (PWAS) to offer insights into the failure evaluation of composite concrete in correlation with AE activity. Details of the methodology, including a concrete test system for AE data acquisition, are thus provided, and the experimental work and its results discussed, allowing some initial conclusions to be drawn.

2. Experimental Work

The experimental section had three parts (a) the preparation of compression specimens with bounded PWAS sensors, (b) data acquisition during compression testing, and (c) data processing.

2.1. Specimens preparation

Two types of specimens were prepared by mixing Portland cement with fine and coarse aggregates and water. Type-A specimens were prepared without reinforcement bars while Type-B specimens included polyamide (Nylon) bars with diameters of 0.8 mm and lengths of 150 mm as reinforcement. Cubic specimens of 150 x 150 x 150 mm were cast in a steel mould and compacted using a tamping rod for compression strength testing.

2.2. Testing procedure

A compressive strength test of the prepared concrete cubes was performed according to BS EN 12390-1 standard [29] using a MATEST machine with a load capacity of 3,000 kN with loads applied at a rate of 0.2 MPa per second. The real time applied loads were recorded using a separate data logger. Eight specimens of cubic concrete, with and without polyamide reinforced bars, were manufactured and tested. A single PWAS sensor was attached to the centre of one side surface of each specimen, as shown in Figure 2a, to monitor specimen damage under compression testing, while the top and bottom surfaces of the specimen were placed between the fixed and moving parts of the testing machine, as shown in Figure 2b. Superglue was used as a mechanical fixture to provide adequate acoustic coupling between the specimen surface and the sensor.

AE activity was recorded throughout testing using a personal laptop with an internal audio card accessed via a 3.5 mm audio jack and coaxial cable as an acquisition system [30]. The twisted pair wire of the sensor was soldered to the coaxial cable wire to prevent any electrical loss during the test. The AE data were captured at a sampling rate of 48 kHz, and a threshold of 0.005 V was considered for all tests, due to conducting the tests in a controlled environment, to remove low-level background noises and electromagnetic noises. The sensor was calibrated using a Hsu Nielson (H-N) fracture source test before each test was conducted [31], done by breaking several pencil leads against the sensor and recording the resulting high amplitude AE signals. The experimental set-up of the testing machine and acquisition system is shown in Figure 2b.

(a) (b)

Figure 2. Test equipment (a) Sensor mounted on the specimen surface (b) Testing machine with acquisition system.

2.3. Data processing

In this study, during each test, the recorded stream was stored on the laptop hard disk for processing in audio file (WAV) format. The minimum and maximum values of the measured amplitude were between -1 and +1 Volt. AE signals were extracted from the recorded stream using the threshold crossing approach: for each AE signal, the AE traditional parameters were extracted using MATLAB R2015a. All essential AE signal features such as arrival time, amplitude, count, rise time and duration were thus extracted.

3. Results and discussion

3.1 Physical observation

Visual inspections were performed on the tested specimens after final failure. Examples of damage on the tested specimens are presented in Figure 3 for both Type-A and Type-B specimens. From the figure, it is clear that both specimen types have surface cracking, though specimens of Type-A exhibited lower signs of damage on the sensor surface compared with specimens of Type-B. All specimens' surfaces showed different levels of damage, however, and visual inspection clearly cannot provide an inspector with a full image of crack development during, or even after, testing. In addition, it does not allow access to assess damage inside the structure or on any inaccessible surfaces, highlighting the need to use structural health monitoring techniques to provide feedback about structural integrity in real-time.

(a) (b)

Figure 3. Final failure of the tested specimens of (a) Type-A and (b) Type-B.

3.2 Acoustic Emission Data analysis:

Figure 4 (a and b) shows the recording of the continuous AE streams for the tested specimens shown in Figure 3. The results show that the test lifetimes for these samples were 137 and 104 seconds for Type-A and Type-B, respectively. As shown in Figure 4a, prior to the 65.7% mark of test life for the Type-A sample, few low amplitude AE events were detected, suggesting there were no severe or detectable cracks occurring within the specimen. However, between 65.7% and 90.5% of the test life, the final failure region was present and AE events were recorded at a rapid rate with several signals of high amplitude. A large accumulative number of events with high event rate can be considered a sign of a burst region [32], and subsequently, small cracks formed quickly based on a continuous increase in the load, with lower AE event amplitudes then showing until the end of the test.

Figure 4b shows that, prior to the 38.5% mark of the test life for the Type-B sample, the AE activity was negligible. However, between 38.5% and 53.5% of the test life, the AE event rate increase significantly, and high amplitude signals were recorded, suggesting the formation of major cracks within the

specimen. AE activity then obviously decreased for the period from 53.5% to 62.5% of the test life. This was followed by an increase in AE activity of high amplitude beginning at approximately 62.5% of the test life and lasting until the end of the test, a period reflecting the fracture process of propagation to final failure.

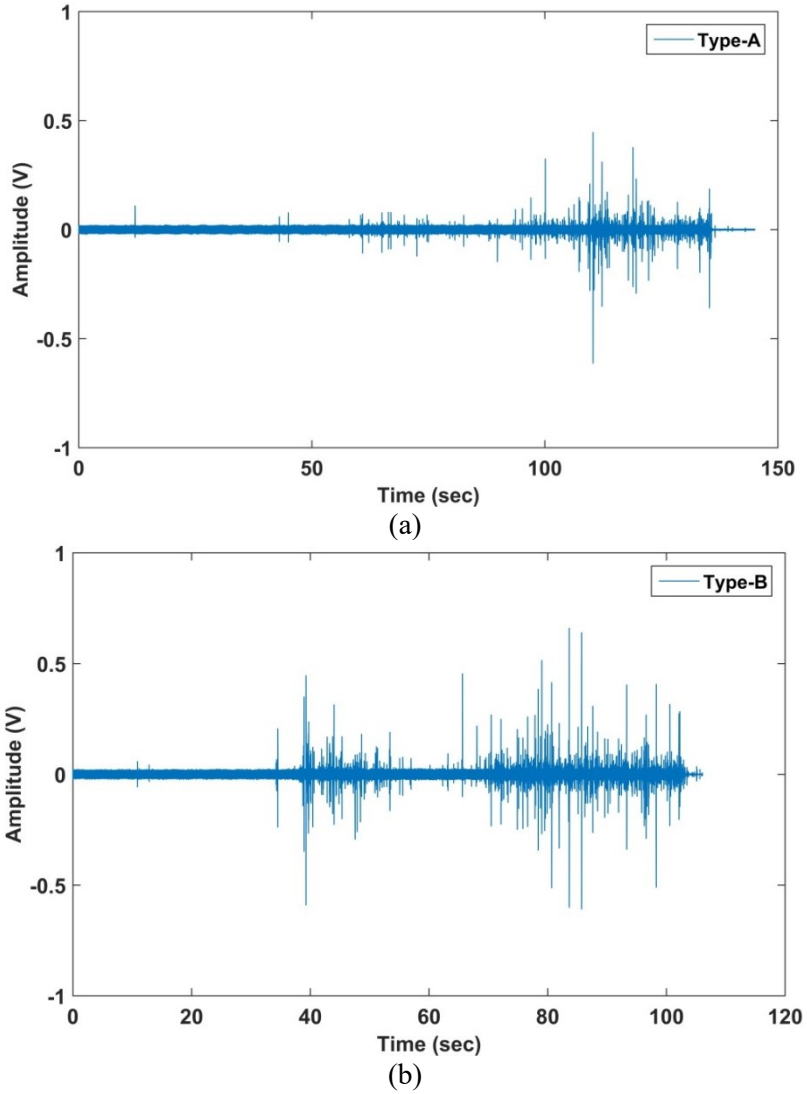

Figure 4. Acquired test data (a) Type-A (b) Type-B.

Figure 5 (a and b) show the loading history diagram of the tested specimens with a superimposition of amplitude value for each AE signal versus time. This shows that the ultimate loads of the Type-A and Type-B specimens are 440.7 and 476 kN, respectively. From Figure 5a, the load begins to rise after 60 seconds from the beginning of the test, an increase that is sustained in a linear manner until about 56.7% of the ultimate load is reached, with only a slight increase in the amplitude of recorded AE signals occurring. After that, the load increases in a curved manner with inconsiderable fluctuation until final failure, an increase most likely associated with recording scattered high amplitude AE signals. However, Figure 5b shows a load that starts to increase after 35 seconds from the start of the test; before this time, there were no detectable high amplitude AE signals in this sample. From the plot of evolution of the load with signal amplitude, it is possible to distinguish two differentiated intervals. The first interval shows that the load increased steadily, with approximately linear behaviour, until reaching about 36% of the ultimate load. During this period, high amplitude AE signals with high intensity were recorded.

The second interval shows the reappearance of high amplitude AE signals with the increase of the load, beginning at about 76% of the ultimate load and lasting until the end of the test.

From Figure 5, the behaviour of the load curve and the corresponding recorded AE activity can be used to distinguish different levels of fracture sources. At the first level, there is no increase in load, with very low AE activity, which may contribute to the friction noise identified between the specimen surface and the compression machine plate. However, at the second level, the load behaviour increases linearly as the elastic zone and AE activity increase, and higher amplitude signals are recorded due to the randomly occurring microcracks. At the third level, the load increases further, and as it reaches the maximum value, the AE hits become much larger, and there is also a significant increase in the event rate. This occurs due to the propagation of major cracks as well as the rapidity of microcrack formation. The specimen must be deemed close to failure at such a point [2, 33].

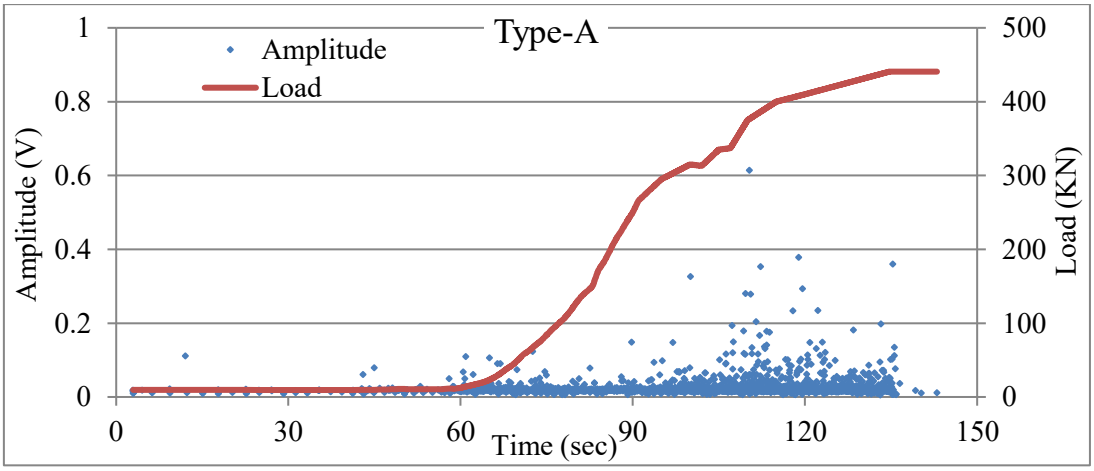

(a)

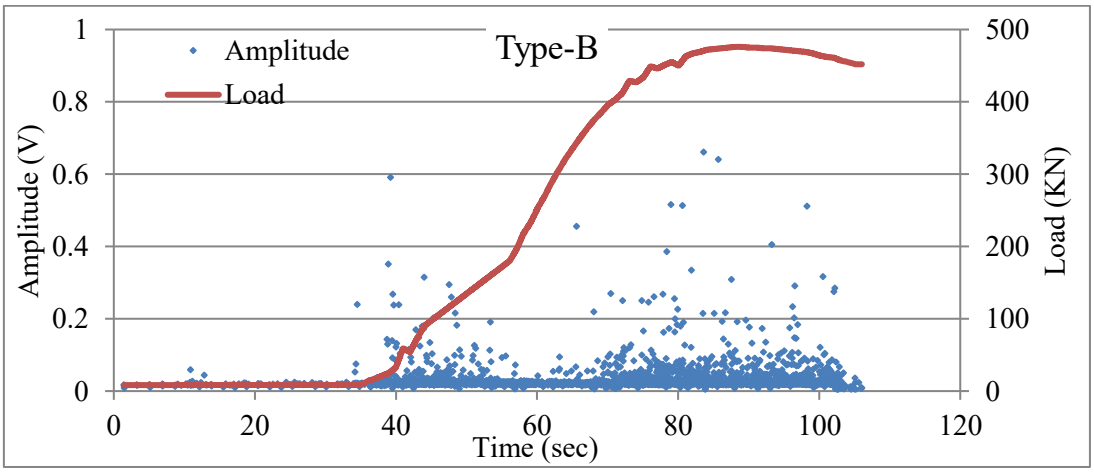

(b)

Figure 5. Amplitude versus load (a) Type-A (b) Type-B.

Figure 6 shows the relationship between cumulative AE hits and the load versus time. Using the setup threshold of 0.005 V, the total number of recorded hits for Type-A and Type-B samples are equal to 3,670 and 3,127, respectively. During AE monitoring, cumulative AE hits associated with load history and other AE parameters, such as signal amplitude, can be used to provide initial information about the structural integrity depending on the rate of release of acoustic waves [30, 34, 35].

Figure 6 (a and b) show the concurrence between AE activity increments and the increase in applied load. As shown, the generation and release of AE hits displays linear behaviour until the end of the test. The low threshold value means that signals of low amplitude, released during micromechanical crack events, represent the majority of the recorded signals. These events represent minor cracks within the loaded structure and have a significant effect on the AE cumulative hits.

A higher threshold of 0.05 V was applied to eliminate the effect of minor cracks on cumulative hits total, and the results for Type-A and Type-B are presented in Figure 6 (c and d), respectively. Here, residual cumulative hits represent approximately 5.15 and 8.72% of the recorded signals for Type-A and Type-B, respectively. For the Type-A specimen, the sharp increase in AE activity in a relatively short period begins at 96 seconds and lasts until the end of the test, while the AE activity in the Type-B specimen showed an obviously sharp increase in two separate periods. The first of these coincided with the first increase in load and lasted for a relatively short period, while the second began at 69 seconds and continued until the end of the test. These signals can thus most likely be classified as intermediate/severe cracks combination.

High energy emissions have been reported as emitted from more severe cracks. Thus, to focus on high amplitude signals only, the cumulative AE hits was recalculated for the 0.1 V threshold, with results as shown in Figure 6 (e and f). The number of cumulative AE hits was reduced to 1.63 and 2.83% of the total recorded signals for Type-A and Type-B specimens, respectively. A sharp increase in AE activity for the Type-A specimen can be seen after 103 seconds, which coincides with 72.6% of the ultimate load, while two sharp increases in activity are shown for the Type-B specimen. The first increase starts simultaneously with the first load increase, whereas the second occurs 70 seconds after the beginning of the test, where the load was 83% of the final failure load. These results agree with the visual observations taken during the tests, and suggest that the initiation of the critical stage of final failure can be identified by means of observing the cumulative hits trend. This methodology can thus be applied to provide feedback about structural integrity and to trigger an alarm at earlier stages of damage, before final failure occurs.

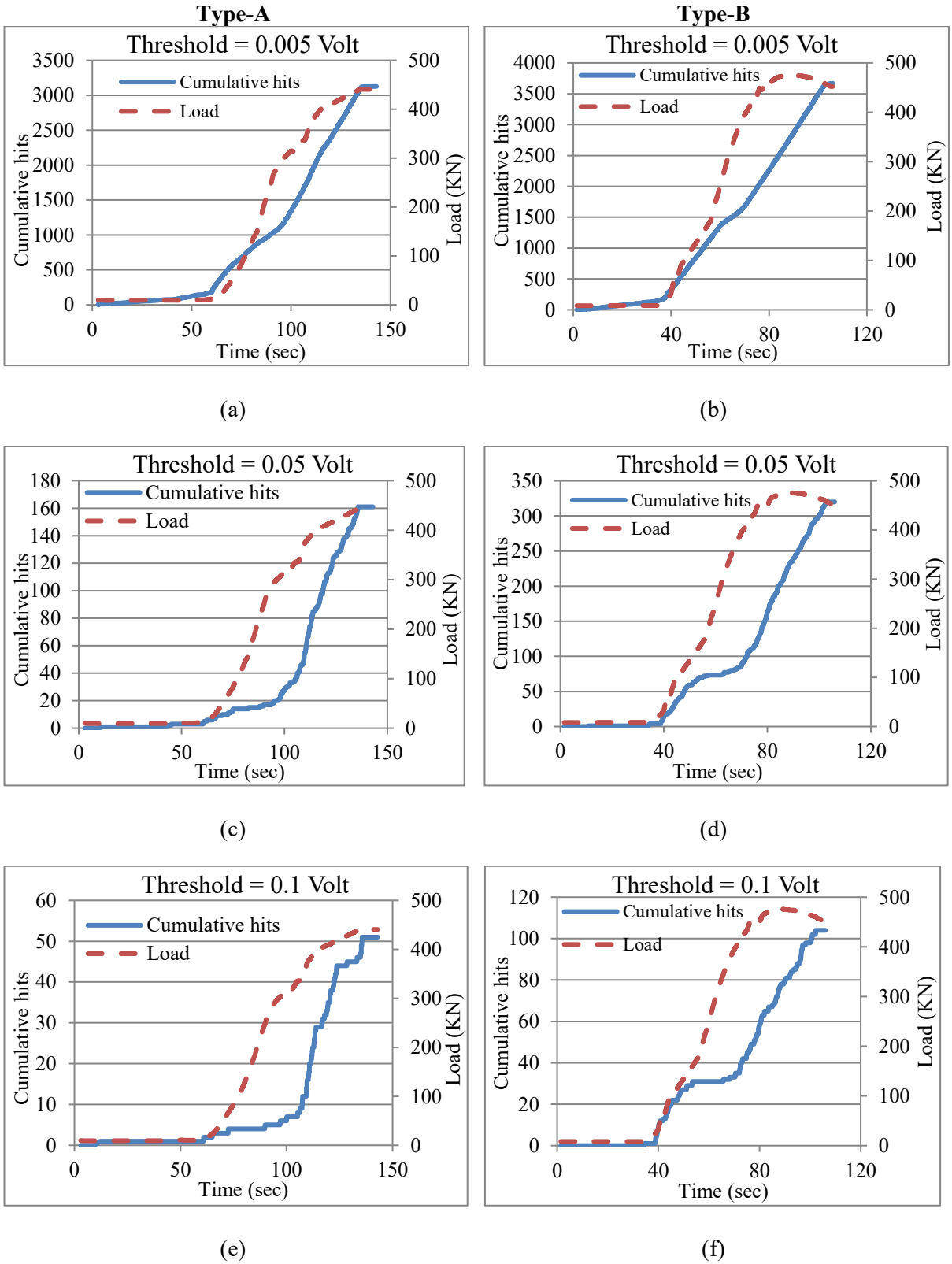

Figure 6. Cumulative AE hits at different threshold levels

4. Conclusions

Real-time low-frequency acoustic emission monitoring was exploited to develop damage evaluation for concrete cube specimens with and without polyamide (Nylon) (Type-A and Type-B) reinforced bars under compression testing. The results showed that the proposed technique can be used for structural health monitoring, and to provide feedback about structural integrity under loading.

The damage evaluation stages and unstable critical state prior to final failure were observed using traditional AE parameters. The initial signs of a final failure stage were detected at loads of 72.6 and 83% of final failure load for Type-A and Type-B specimens, respectively.

Although the technique used is limited with respect to frequency coverage, it may be used widely in situ due to low storage and application costs and acceptable results. Furthermore, the proposed technique may also be used effectively to correlate signal feature-based characterisations of AE sources in applications of non-destructive testing.

5. References

[1] Shah A A and Hirose S 2010 Nonlinear ultrasonic investigation of concrete damaged under uniaxial compression step loading *Journal of Materials in Civil Engineering* **22** 476-84
[2] Habib M A, Rai A and Kim J-M 2020 Performance Degradation Assessment of Concrete Beams Based on Acoustic Emission Burst Features and Mahalanobis—Taguchi System *Sensors* **20** 3402
[3] Giurgiutiu V 2007 *Structural health monitoring: with piezoelectric wafer active sensors*: Elsevier)
[4] Duan W H, Wang Q and Quek S T 2010 Applications of piezoelectric materials in structural health monitoring and repair: Selected research examples *Materials* **3** 5169-94
[5] Liao W-I, Wang J, Song G, Gu H, Olmi C, Mo Y, Chang K and Loh C 2011 Structural health monitoring of concrete columns subjected to seismic excitations using piezoceramic-based sensors *Smart Materials and Structures* **20** 125015
[6] Shi Y, Luo M, Li W and Song G 2018 Grout compactness monitoring of concrete-filled fiber-reinforced polymer tube using electromechanical impedance *Smart Materials and Structures* **27** 055008
[7] Yapar O, Basu P, Volgyesi P and Ledeczi A 2015 Structural health monitoring of bridges with piezoelectric AE sensors *Engineering Failure Analysis* **56** 150-69
[8] Sagasta F, Zitto M E, Piotrkowski R, Benavent-Climent A, Suarez E and Gallego A 2018 Acoustic emission energy b-value for local damage evaluation in reinforced concrete structures subjected to seismic loadings *Mechanical Systems and Signal Processing* **102** 262-77
[9] Verstrynge E, De Wilder K, Drougkas A, Voet E, Van Balen K and Wevers M 2018 Crack monitoring in historical masonry with distributed strain and acoustic emission sensing techniques *Construction and Building Materials* **162** 898-907
[10] Miller K R and Hill E K 2005 *Nondestructive Testing Handbook, Acoustic Emission Testing* vol 6
[11] Crivelli D, Guagliano M, Eaton M, Pearson M, Al-Jumaili S, Holford K and Pullin R 2015 Localisation and identification of fatigue matrix cracking and delamination in a carbon fibre panel by acoustic emission *Composites Part B: Engineering* **74** 1-12
[12] Al-Jumaili S K, Pearson M, Holford K M, Eaton M J and Pullin R 2016 Fast and Reliable Acoustic Emission Source Location Technique in Complex Structures. In: *24th UK Conference of the Association for Computational Mechanics in Engineering (ACME-UK),* (Cardiff, UK

[13] Al-Jumaili S K, Pearson M R, Holford K M, Eaton M J and Pullin R 2016 Acoustic emission source location in complex structures using full automatic delta T mapping technique *Mechanical Systems and Signal Processing* **72–73** 513-24
[14] Kundu A, Eaton M, Al-Jumali S, Sikdar S and Pullin R 2017 Acoustic emission based damage localization in composites structures using Bayesian identification. In: *Proceedings of the 12th International Conference on Damage Assessment of Structures (DAMAS), Kitakyushu, Japan,* pp 10-2
[15] Al-Jumaili S K, Holford K M, Eaton M J, McCrory J P, Pearson M R and Pullin R 2014 Classification of acoustic emission data from buckling test of carbon fibre panel using unsupervised clustering techniques *Structural Health Monitoring*
[16] Al-Jumaili S K, Eaton M J, Holford K M, Pearson M R, Crivelli D and Pullin R 2016 Characterisation of Fatigue Damage in Composites Using an Acoustic Emission Parameter Correction Technique *Composites Part B: Engineering*
[17] Sshrama K, Al-Jumaili S K, Pullin R, Clarke A and Evans S 2019 On the use of acoustic emission and digital image correlation for welded joints damage characterization *Journal of Applied and Computational Mechanics* **5** 381-9
[18] Huang M, Jiang L, Liaw P K, Brooks C R, Seeley R and Klarstrom D L 1998 Using acoustic emission in fatigue and fracture materials research *Jom* **50** 1-14
[19] Das A K, Suthar D and Leung C K 2019 Machine learning based crack mode classification from unlabeled acoustic emission waveform features *Cement and Concrete Research* **121** 42-57
[20] Yu X, Bentahar M, Mechri C and Montrésor S 2019 Passive monitoring of nonlinear relaxation of cracked polymer concrete samples using Acoustic Emission *The Journal of the Acoustical Society of America* **146** EL323-EL8
[21] Aggelis D, De Sutter S, Verbruggen S, Tsangouri E and Tysmans T 2019 Acoustic emission characterization of damage sources of lightweight hybrid concrete beams *Engineering Fracture Mechanics* **210** 181-8
[22] Banjara N K, Sasmal S and Srinivas V 2019 Investigations on acoustic emission parameters during damage progression in shear deficient and GFRP strengthened reinforced concrete components *Measurement* **137** 501-14
[23] Yue J, Kunnath S and Xiao Y 2020 Uniaxial concrete tension damage evolution using acoustic emission monitoring *Construction and Building Materials* **232** 117281
[24] Chen C, Fan X and Chen X 2020 Experimental investigation of concrete fracture behavior with different loading rates based on acoustic emission *Construction and Building Materials* **237** 117472
[25] OHTSU M 1992 Rate process analysis of acoustic emission activity in core test of concrete *Doboku Gakkai Ronbunshu* **1992** 211-7
[26] Ohtsu M and Watanabe H 2001 Quantitative damage estimation of concrete by acoustic emission *Construction and Building Materials* **15** 217-24
[27] Huo L, Cheng H, Kong Q and Chen X 2019 Bond-slip monitoring of concrete structures using smart sensors—A review *Sensors* **19** 1231
[28] Soh C K, Tseng K K, Bhalla S and Gupta A 2000 Performance of smart piezoceramic patches in health monitoring of a RC bridge *Smart materials and Structures* **9** 533
[29] Standard B 2009 Testing hardened concrete *Compressive Strength of Test Specimens, BS EN* 12390-3
[30] Negi P and Chakraborty T 2020 Acquisition of Acoustic Emission Signals from Rocks Using Directly Bonded PZT Patches *Indian Geotechnical Journal* **50** 117-32
[31] Hsu N N and Breckenridge F R 1981 Characterization and Calibration of Acoustic Emission Sensors. *Materials Evaluation* **39** 60-8
[32] Lu Y and Li Z 2008 *Earth & Space 2008: Engineering, Science, Construction, and Operations in Challenging Environments,* pp 1-11

[33] Aldahdooh M and Bunnori N M 2013 Crack classification in reinforced concrete beams with varying thicknesses by mean of acoustic emission signal features *Construction and Building Materials* **45** 282-8
[34] Shah A A, Ali R, Naseer A and Zhang C 2014 Assessment of Progressive Damages in Concrete with Acoustic Emission Technique *Advances in Applied Acoustics (AIAAS)* **3**
[35] Sagar R V 2017 Acoustic emission characteristics of reinforced concrete beams with varying percentage of tension steel reinforcement under flexural loading *Case studies in construction materials* **6** 162-76